

Real-time analysis of organic compounds in ship engine aerosol emissions using resonance-enhanced multiphoton ionisation and proton transfer mass spectrometry

Christian Radischat · Olli Sippula · Benjamin Stengel ·
Sophie Klingbeil · Martin Sklorz · Rom Rabe ·
Thorsten Streibel · Horst Harndorf · Ralf Zimmermann

Received: 12 November 2014 / Revised: 28 December 2014 / Accepted: 5 January 2015 / Published online: 20 January 2015
© Springer-Verlag Berlin Heidelberg 2015

Abstract Organic combustion aerosols from a marine medium-speed diesel engine, capable to run on distillate (diesel fuel) and residual fuels (heavy fuel oil), were investigated under various operating conditions and engine parameters. The online chemical characterisation of the organic components was conducted using a resonance-enhanced multiphoton ionisation time-of-flight mass spectrometer (REMPI TOF MS) and a proton transfer reaction-quadrupole mass spectrometer (PTR-QMS). Oxygenated species, alkenes and aromatic hydrocarbons were characterised. Especially the aromatic hydrocarbons and their alkylated derivatives were very

prominent in the exhaust of both fuels. Emission factors of known health-hazardous compounds (e.g. mono- and poly-aromatic hydrocarbons) were calculated and found in higher amounts for heavy fuel oil (HFO) at typical engine loadings. Lower engine loads lead in general to increasing emissions for both fuels for almost every compound, e.g. naphthalene emissions varied for diesel fuel exhaust between 0.7 mg/kWh (75 % engine load, late start of injection (SOI)) and 11.8 mg/kWh (10 % engine load, late SOI) and for HFO exhaust between 3.3 and 60.5 mg/kWh, respectively. Both used mass spectrometric techniques showed that they are particularly suitable methods for online monitoring of combustion compounds and very helpful for the characterisation of health-relevant substances.

Published in the topical collection *Aerosols and Health* with guest editor Ralf Zimmermann.

C. Radischat · S. Klingbeil · M. Sklorz · T. Streibel (✉) ·
R. Zimmermann

Joint Mass Spectrometry Centre/Chair of Analytical Chemistry,
University of Rostock, 18051 Rostock, Germany
e-mail: Thorsten.Streibel@uni-rostock.de

M. Sklorz · T. Streibel · R. Zimmermann
Cooperation Group Comprehensive Molecular Analytics, Helmholtz
Zentrum München, Deutsches Forschungszentrum für Gesundheit
und Umwelt (GmbH), 85764 Neuherberg, Germany

B. Stengel · R. Rabe · H. Harndorf
Faculty of Mechanical Engineering and Marine Technology, Chair of
Piston Machines and Internal Combustion Engines, University of
Rostock, 18059 Rostock, Germany

O. Sippula
Department of Environmental Science, University of Eastern
Finland, 70101 Kuopio, Finland

C. Radischat · O. Sippula · B. Stengel · S. Klingbeil · T. Streibel ·
R. Zimmermann
Helmholtz Virtual Institute of Complex Molecular Systems in
Environmental Health (HICE)—Aerosols and Health, Helmholtz
Zentrum München, Deutsches Forschungszentrum für Gesundheit
und Umwelt (GmbH), 85764 Neuherberg, Germany

Keywords Ship emissions · Poly-cyclic aromatic
hydrocarbons · REMPI TOF MS · Heavy fuel oil · Diesel fuel

Introduction

Increasing ship traffic and resulting increased gas phase and particular phase exhaust emissions lead to a higher concern about the effects of that emission source. Ship emissions are suspected to have a direct impact on climate conditions and the health of humans [1–5]. Especially the exhaust gas components carbon monoxide (CO), HC, nitrogen oxides (NO_x), sulphur dioxide (SO₂) and particulate matter (PM) account for a large proportion of emitted exhaust species [5–9]. Due to the high emissions, reduction protocols have been introduced, e.g. the sulphur content of the used fuels is limited by regulations of *The International Convention for the Prevention of Marine Pollution from Ships, 1973 (MARPOL 73/78)*. A relatively

new measure is the institution of SO_x emission control areas (SECAs) in epicontinental seas such as the Baltic and the North Sea. In such areas, the maximum fuel sulphur content of 0.1 % must not be exceeded from 2015 onwards. The sulphur content regulations will lead to the usage of low sulphur marine diesel fuels instead of heavy fuel oils in the SECAs. This fuel change will also affect largely the polycyclic aromatic hydrocarbon (PAH) emissions, which are considered as health hazardous and, therefore, are of particular importance [10, 11].

Until now, PM emissions of marine vessels have been characterised mainly in terms of size distribution and chemical composition of the particles [11–15]. However, the complex interaction of particulate and gaseous phase requires also a detailed description of the organic trace components in the gas phase of fuel exhaust. One possible way to achieve this is characterisation of organic gas phase content via the sum parameter total hydrocarbons (THC) [16]. There are some articles about the determination of organic gaseous exhaust emissions of automobile diesel engines [16, 17] and marine engines [10, 18] using offline grab sample techniques dealing mainly with the investigation of PAH, but there are only very few reports [19] about online sampling and monitoring methods as well as real-time exhaust gas measurements [20–22]. In general, there is a lack of knowledge about online characterisation and monitoring of marine vessel exhaust at different engine loads and various operation parameters. Moreover, in comparison to on-road exhaust emissions, there is only little knowledge about the exhaust characterisation of maritime vessels using heavy fuel oil. Until now, there are no measurements dealing with online characterisation of gas phase organic compounds at marine engines.

Exhaust emissions are generally dependent on the engine parameters and operating modes [23, 24]. The tested four-stroke single cylinder research engine represents a typical modern medium-speed diesel engine, which is capable to run on both residual and distillate fuels. Therefore, this study investigates the chemical characterisation of organic trace components from a research engine at different loads and engine parameters using different fuels (diesel and heavy fuel oil (HFO)). The exhaust gas, containing regulated and unregulated engine emissions, was sampled directly in the exhaust pipe using a proton transfer reaction-quadrupole mass spectrometer (PTR-QMS), a resonance-enhanced multiphoton ionisation time-of-flight mass spectrometer (REMPI TOF MS) and commercially available gas analysers (AVL CEB II). The latter monitor bulk combustion gases such as CO , NO_x and SO_2 as well as the organic sum parameter of THC. With the aid of known relative ionisation cross sections, a semi-quantification of some selected oxygenated, monoaromatic and polyaromatic compounds was performed and emission factors were calculated.

This study was carried out as part of a project of the Helmholtz Virtual Institute for Complex Molecular Systems in Environmental Health—Aerosols and Health (HICE). Within the HICE Virtual Institute, the health effects of combustion aerosol emissions are studied by comprehensive analysis of the combustion aerosols and the molecular biological effects of the emissions on human lung cell cultures exposed at the air liquid interface. In this framework, the here presented study of the application of two different online mass spectrometry methods to ship diesel engine emissions has been conducted.

Experimental section

All ship engine emission measurements were performed at the Chair of Piston Machines and Internal Combustion Engines at the University of Rostock, Germany. For the investigation of diesel fuel (DF) according to EN 590 and HFO exhaust, a single cylinder research engine (1 VDS 18/15 CR) capable to run on both fuels was used. The layout of the engine represents a typical modern medium-speed marine diesel engine with charge air supply and a common rail injection system. Though the engine has a maximum output of 80 kW, its combustion processes are comparable to those of full engines. Table 1 summarises the parameters of the research engine.

For the exhaust gas measurements, the engine was operated at constant speed (1500 min^{-1}) but varying loads between idling and 100 % of maximum output. For every load, two different starts of injection (SOI) were set, an early and a late injection for each of the two fuels. The late SOI represents a typical real scenario working point, whereas the early SOI describes a low soot-producing case. In general, SOI describes the position of the piston at the beginning of fuel injection.

On the one hand, a common diesel fuel according to the DIN EN 590 standard, which limits the sulphur content in the fuel to a maximum 0.001 %, and on the other hand, a heavy fuel oil with a sulphur content of 2.7 % were used. The fuel properties of both fuels can be found in Table 2.

Table 1 Research engine specifications

Engine designation	1 VDS 18/15 CR
Operation mode	Four stroke diesel, direct injected, compressor charged
Number of cylinders	1
Valves	4
Stroke volume	180 mm
Bore	150 mm
Connecting rod length	332 mm
Nominal speed	1500 min^{-1}
Maximum output	80 kW

Table 2 Fuel properties of diesel fuel (DIN EN 590) and heavy fuel oil 380

Parameter	Test specification	Value
Flash point [°C]	ISO 2719	67 ^a
Density at 15 °C [g/L]	DIN EN ISO 12185	842.5 ^a
Viscosity at 40 °C [mm ² /s]	DIN 53015	3.3 ^a
Heating value [MJ/kg]	DIN 51900-2	35.8 ^a
Water content [mg/kg]	EN ISO 12937	80 ^a
Carbon content [wt%]	DIN 51732	86.5 ^a
Hydrogen content [wt%]	DIN 51732	13.4 ^a
Flash point [°C]	ISO 2719	128 ^b
Density at 15 °C [g/L]	DIN EN ISO 12185	995 ^b
Viscosity at 50 °C [mm ² /s]	ASTM D 7042	180.7 ^b
Sulphur content [% (m/m)]	DIN 51400-10	2.7 ^b
Heating value [MJ/kg]	DIN 51900-1, 51900-3	39.5 ^b
Water content [wt%]	EN ISO 12937	0.53 ^b
Carbon content [wt%]	DIN 51732	84.39 ^b
Hydrogen content [wt%]	ISO 12937	10.52 ^b

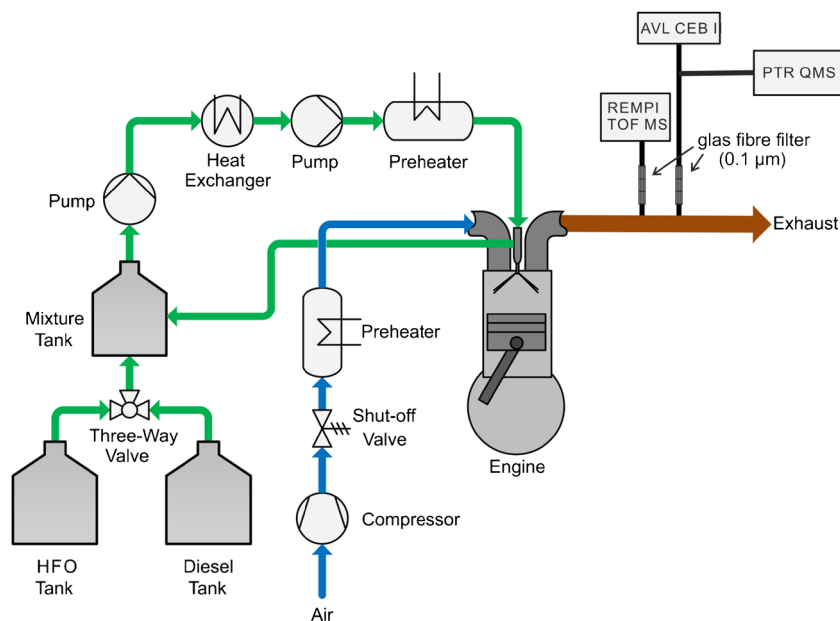
^a Diesel (DIN EN 590)^b HFO 380

Raw gas sampling for REMPI TOF MS was carried out using a 300 °C heated glass fibre filter (pore diameter 0.1 µm) and a capillary interface heated to 300 °C. PTR-QMS and gas analysers were coupled by a 180 °C heated stainless steel transfer line with a built-in particle filter. A schematic overview of the engine and the used systems can be found in Fig. 1.

REMPI TOF MS technique was utilised for a selective detection of aromatic hydrocarbons. The REMPI operation

is a two-step ionisation process using ultraviolet (UV) photons to exceed the ionisation energies of the investigated compounds. A detailed description of that process can be found in [25, 26]. Generation of UV photons was carried out by the fourth harmonic (266 nm, 4.66 eV) of a Nd:YAG laser (Big Sky Ultra, Quantel, Les Ulis, France) with a 10-Hz repetition rate, a pulse width of 10 ns and a power density of approximately 7×10^6 W/cm². The applied wavelength is highly selective for aromatic compounds; however, the individual ionisation cross sections may differ greatly [27]. The unfocused beam was guided into the ion source of a reflectron time-of-flight mass spectrometer (CTF 10, Kaesdorf Geräte für Forschung und Industrie, Munich, Germany). Transfer of the components into the mass spectrometer was done, with a constant flow of 4 ml/min, using a deactivated silica capillary (length 1.5 m; i.d. 200 µm; o.d. 350 µm), which run inside a heated transfer line. The calculated mass resolution of the used REMPI TOF MS is $R_{50\%} = 650$ at m/z 112.

For semi-quantification of some selected exhaust components with the REMPI technique, the ionisation efficiencies of these substances must be known. For this reason, relative REMPI cross sections of phenol, naphthalene, methyl naphthalene, phenanthrene and pyrene were determined in laboratory experiments with the same mass spectrometer utilised for the online and real-time exhaust emission measurements. The ionisation cross section of toluene was set by definition to one and those of the other compounds were calculated in relation to toluene by comparing their respective signal intensities relative to toluene. A detailed description of such a cross section determination can be found in [21]. It was assumed that the ion signals at m/z 178 and m/z 202 belong almost

Fig. 1 Schematic layout of the single cylinder medium-speed marine diesel research engine with charge air supply and common rail injection system

solely to phenanthrene and pyrene, respectively, because the isomers anthracene and fluoranthene have REMPI cross sections that are smaller by several orders of magnitude in comparison to phenanthrene and pyrene [21].

Detection of volatile organic compounds was carried out by a PTR-QMS (Ionicon Analytik GmbH, Innsbruck, Austria). In the present study, the drift chamber was operated at a pressure of 2.0 mbar, a temperature of 60 °C and a drift voltage of 600 V. The pressure in the mass analyser was 5×10^{-5} mbar. The system operated with unit mass resolution in scan mode with a dwell time of 0.1 s for each nominal mass. For the transport of gas phase components into the mass spectrometer, a homemade interface was used. In brief, a deactivated fused silica capillary (length 2 m; i.d. 530 μm) in a heated transfer line (100 °C) has been installed to reduce sample flow to about 50 ml/min and prevent condensation [28]. PTR-MS is a chemical ionisation technique, where the primary ions (H_3O^+) were produced in the ion source with the aid of a hollow cathode discharge using water vapour as reactant gas. The technique is based on non-dissociative proton transfer reaction between the hydronium ions and neutral molecules in the drift tube and forms protonated molecule ions and water. The reaction only occurs if the neutral molecules have higher proton affinities than water. Bulk components such as oxygen, nitrogen, carbon monoxide and carbon dioxide cannot be ionised due to their lower proton affinities in comparison to water. A detailed description of the PTR-MS technique can be found in [29–31].

The gas analyser, AVL CEB II, was utilised for measurements of main exhaust pollutants, such as CO, carbon dioxide (CO_2), nitrogen oxides (NO_x), THC and SO_2 , and it was coupled directly to the 180 °C heated stainless steel transfer line.

Data acquisition and processing of the REMPI data was carried out with custom-made LabView (National Instruments Corporation, Austin, TX) software and Aquiris AP 240 (Agilent Technologies, USA) averager cards with associated software. MatLab R2010b (MathWorks) was used for further statistical evaluations. For PTR-MS data acquisition and processing, Quadstar 32 BIT 7.03 software was applied and further statistical evaluations were also done with MatLab R2010b (MathWorks).

The mass spectrometric REMPI data have a time resolution of 1 s per spectrum, whereas the PTR-QMS data recording took 24 s for one full scan mass spectrum due to the recorded mass range of 240 nominal masses and the 0.1-s dwell time for each mass in the observed mass range.

Results and discussion

Compound assignment is in some cases difficult because of the possibility of two or more substances for the same nominal mass to charge ratio. Nevertheless, by comparison to published offline literature about diesel fuel exhaust [16, 17, 19, 32, 33] and ship emissions [12, 18, 34] as well as knowledge about relative ionisation cross sections for 266 nm REMPI, it is feasible to allocate the compounds in a first approximation.

The engine was always started with diesel fuel, and after about 30 min, the fuel was changed slowly to HFO. Figure 2 illustrates a typical engine start-up procedure depicting time traces of some volatile and semi-volatile organic compounds. In the lower mass range between m/z 92 and m/z 142, one can observe a short yet steep increase in concentration, shortly after cold engine start with diesel fuel. Almost all compounds in the higher mass range up to m/z 250 occur slightly later, indicating the formation of these compounds with the onset and progression of combustion. The change of the used fuel from diesel fuel operation to HFO operation leads to a significant increase of almost all poly-aromatic compounds in the observed mass range and a shift to slightly larger compounds such as phenanthrene and pyrene and its alkylated derivatives. Only the mono-aromatic compounds toluene and xylenes remain unaffected by this increase, with the exception of a small peak emission appearing at the same time as the maxima of the PAH emissions. Especially for the mono-aromatic compounds at m/z 120, 134 and 148, even a slight decrease in intensity can be observed. The unburned HFO contains only little or no mono-aromatic hydrocarbons (MAHs) due to the high boiling temperature of the main components. Therefore, the obtained signals are mainly composed of burned and partially oxidised fuel components. On the other hand, the content of MAHs in DF is much higher, and therefore, the signals are derived as a mixture of unburned and thermally decomposed mono-aromatic fuel components and PAHs such as naphthalene and its alkylated derivatives. In reverse, the high content of PAHs in HFO in comparison to DF leads to the increase of that compound class in the emission pattern once the fuel change happened.

As explained above, the signal at m/z 178 relates almost solely to phenanthrene because of its much higher relative ionisation cross section at a laser wavelength of 266 nm compared to anthracene [21]. In addition to that fact, much higher emission rates were measured for phenanthrene in earlier publications [12, 17, 18].

Figure 3 shows once more the complexity of exhaust gases with signals of aromatic species at almost every even mass in a range between m/z 78 and m/z 300. All spectra show approximately the same pattern, with varying signal intensities of individual m/z values, e.g. the peaks for mono-aromatic hydrocarbons at m/z 92, 106, 120 and 134, which are clearly visible in DF exhaust, but less prominent for HFO exhaust.

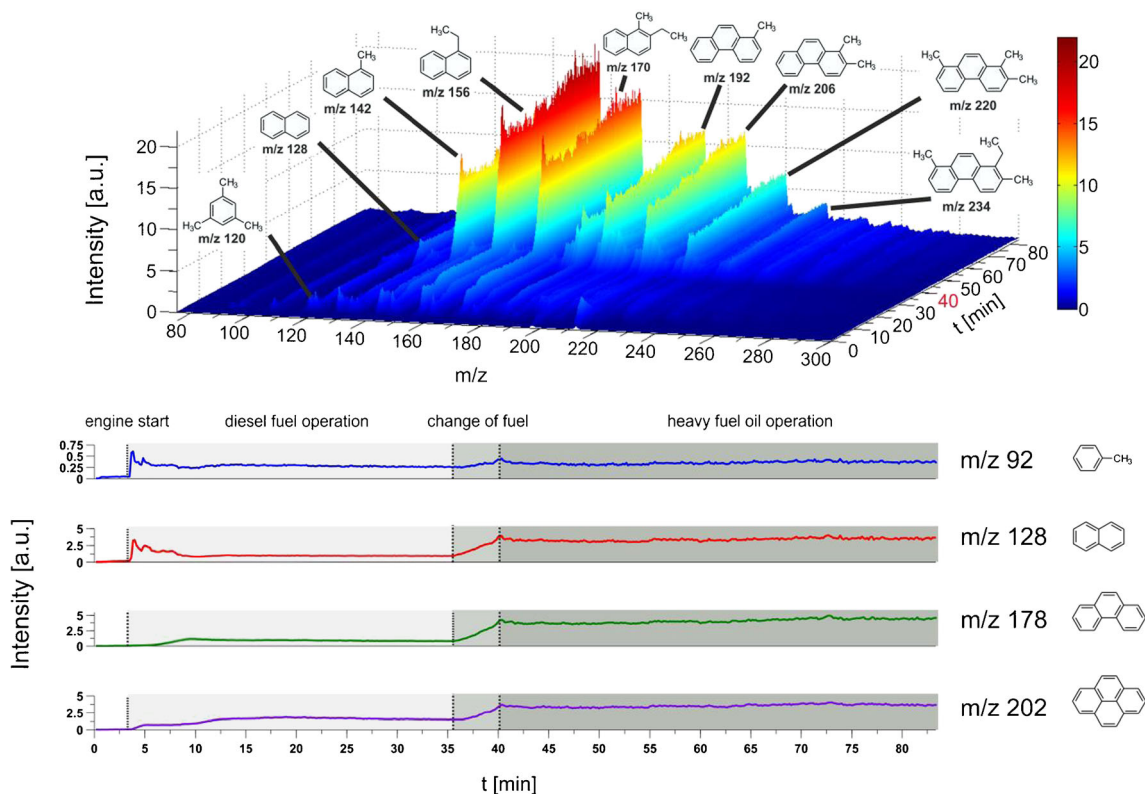


Fig. 2 Top: three-dimensional time-resolved REMPI data over 85 min of all mono- and poly-aromatic compounds in a mass range between m/z 75 and m/z 300 with engine start, after start-up diesel fuel operation at 50 % (40 kW) load and 1500 rpm for 32 min followed by a change to HFO

conditions and stable HFO operation at the same conditions. Bottom: corresponding time-resolved data of toluene, naphthalene, phenanthrene and pyrene

The eight mass spectra shown in Fig. 3 were selected to demonstrate the range of variability between high and low engine loads as well as early and late SOI, respectively. At high power (60 kW (75 %)) conditions for DF operation, the signals at m/z 156 and 170 appear with the highest intensities and can be assigned to the C₂- and C₃-alkylated naphthalene derivatives. This also holds true for maximum (80 kW (100 %)) and intermediate power (40 kW (50 %)) and 20 kW (25 %). For low power (8 kW (10 %)) and idling conditions, one can observe increasing signal intensity for naphthalene and its mono-alkylated derivative at m/z 128 and 142. The same holds true for HFO conditions (high (75 %) and intermediate (25 %) power). Only at low power (10 %) HFO operation conditions, the spectra show different behaviours, depicting methyl phenanthrene (m/z 192) and the C₂-alkylated phenanthrenes (m/z 206) with highest intensities.

The overview on the DF mass spectra shows no big differences between an early and late injection, with the exception of low power conditions, where the intensities of almost all compounds are slightly higher (e.g. factor of 1.5 to 2 for 10 % engine load) for late injection in comparison to early injection. One possible reason could be the poorer and more instable combustion at low load levels caused by lower combustion temperatures, which gives rise to a more incomplete

combustion. Increasing values for carbon monoxide also corroborates a poorer combustion at low load levels, viz. 0.4 g/kWh at maximum power in comparison to 14.8 and 18.9 g/kWh at low power conditions for early and late injection, respectively, which is a typical behaviour of diesel engines [24]. The sum parameter of THC also shows an increase in emission factors for low loads (3.5 and 8.4 g/kWh) in comparison to high engine loads (0.9 g/kWh).

Running the engine with diesel fuel at 80 kW (100 %) operation for early injection and 60 kW (75 %) operation for early and late injection point, respectively, there is a relatively high signal at m/z 202 which can be assigned to pyrene (see above for details of the assignment). The relatively high intensities of pyrene at maximum and high engine power can be caused by high combustion temperatures and the resulting displacement of the gas phase/particle phase equilibrium. It is known that pyrene occurs both in the gas and the particle phase. Schauer et al. [17] reported in their study that 55.2 % of the total pyrene quantity occurs in the particulate phase and 44.8 % in the gaseous phase, respectively.

Benzofuran (m/z 118) and its alkylated derivatives also appear with high intensities in diesel fuel exhaust with the highest signal intensities for C₂- and C₃-alkylated derivatives

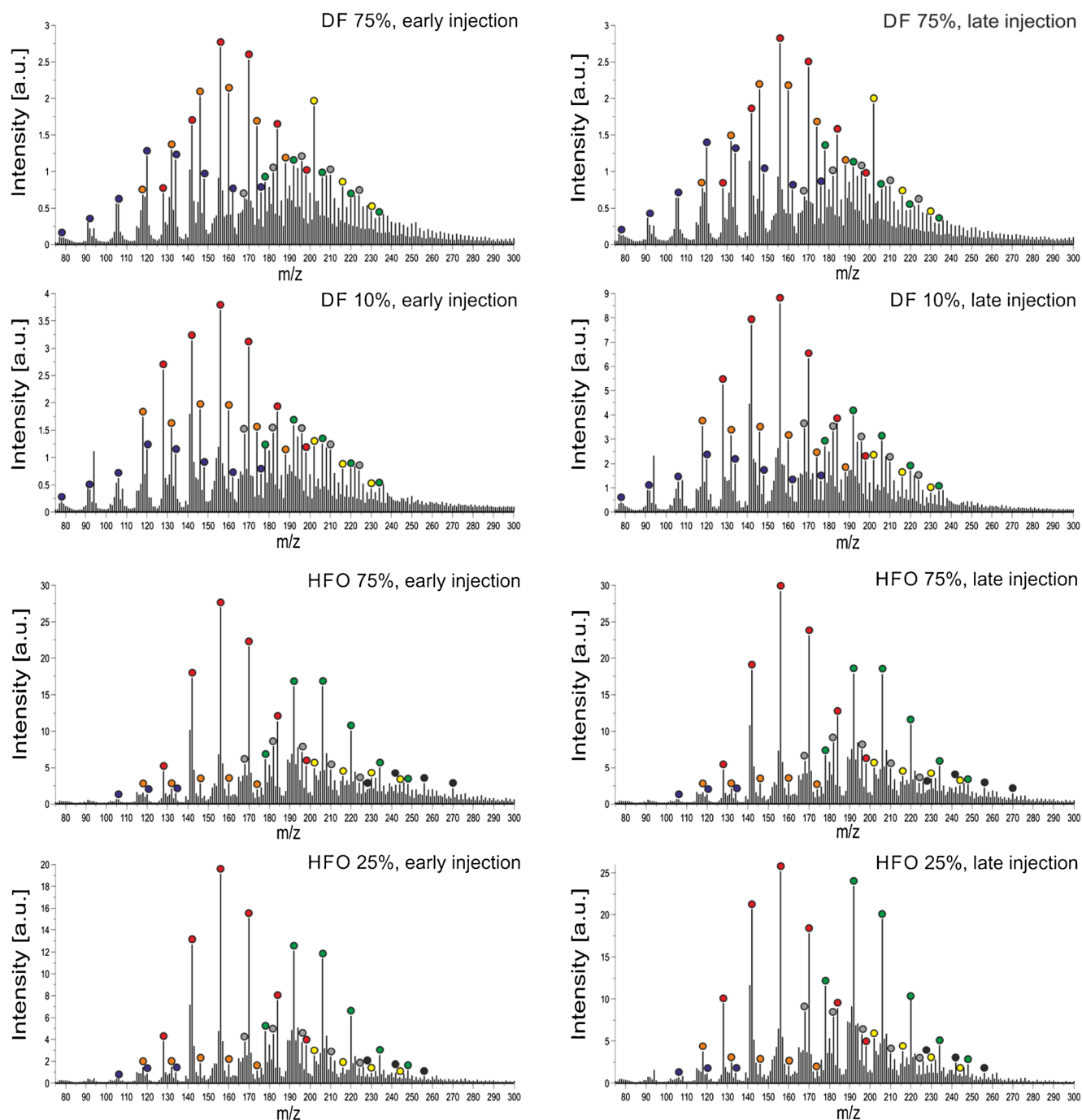


Fig. 3 REMPI mass spectra of DF (75 and 10 % engine power) and HFO (75 and 25 % engine power) exhaust for early and late injection averaged over 1000 s at stable operation conditions. *Blue circles*—homologous series of benzene, *orange circles*—homologous series of benzofuran, *red*

circles—homologous series of naphthalene, *grey circles*—homologous series of dibenzofuran, *green circles*—homologous series of phenanthrene, *yellow circles*—homologous series of pyrene, *black circles*—homologous series of chrysene and/or benz[*a*]anthracene

of that compound. For these compounds, one can observe a changing pattern. On the one hand, the amount of benzofuran increases with decreasing engine power, and on the other hand, there is a decrease of m/z 160 with decreasing loads.

The mass spectrometric pattern of heavy fuel oil exhaust looks a little bit different in comparison to diesel fuel exhaust, due to the fact that the homologous row of phenanthrene and

its alkylated derivatives (m/z 178, 192, 206, 220, 234) appear with much higher signal intensities than for DF exhaust. The comparison of the total ion current (TIC) in the mass range from m/z 75 to m/z 300 results in generally higher values for HFO with a variation by a factor of 2.7 to 7.3. The largest differences occur at high and low load levels of the engine, e.g. a factor of 6.2 at 75 % with late injection and 6.0 and 7.3 at

25 and 10 %, respectively. Poly-aromatic compounds (e.g. naphthalene, phenanthrene, pyrene and each of their alkylated homologs) show significant differences in signal intensity in contrast to mono-aromatic compounds (e.g. toluene, phenol and trimethyl benzene), which show only minor differences in signal intensity. With some of the latter compounds, there are higher emission intensities for diesel fuel exhaust than for heavy fuel oil exhaust, e.g. trimethyl benzene at 50 % load (early and late injection) with a factor of 1.7 and 1.6, respectively. This is due to the higher amount of mono-aromatics in unburned diesel fuel in comparison to HFO. On the other hand, the amount of poly-cyclic aromatic compounds in unburned HFO is higher than in DF. Sippula et al. [11] also showed in their study the larger amount for selected PAHs in HFO in comparison to diesel fuel. At lower combustion temperatures (lower engine loads), the proportion of unburned fuel which leaves the combustion chamber is higher than for high engine loads.

For the poly-aromatic compounds naphthalene and phenanthrene, there is a dominance of their alkylated derivatives compared to the unalkylated species. In most cases, C₁-, C₂- and C₃-alkylated derivatives exhibit the highest signal intensities for both fuels. A normalisation of the appearing signals was conducted. The sum of the signal intensities within the homologous rows from the unalkylated to the C₅-alkylated species was set to 100 %. On the one hand, a slight increase of the relative intensity of naphthalene and methyl naphthalene was observed for low power conditions, and on the other hand, there was a decrease of the higher alkylated derivatives. Only the dimethyl/ethyl naphthalene remains approximately constant at all different engine loads. That also may be due to the fact of decreasing exhaust temperatures with decreasing loads, taking into account the increasing boiling point of compounds with a higher degree of alkylation. A decreasing combustion temperature is combined with a changing ratio of thermally decomposed to unburned fuel. There are especially in unburned diesel fuel comparatively high values for

Fig. 4 Stacked barplots of naphthalene, phenanthrene and pyrene up to their C₅-alkylated derivatives each from DF and HFO exhaust

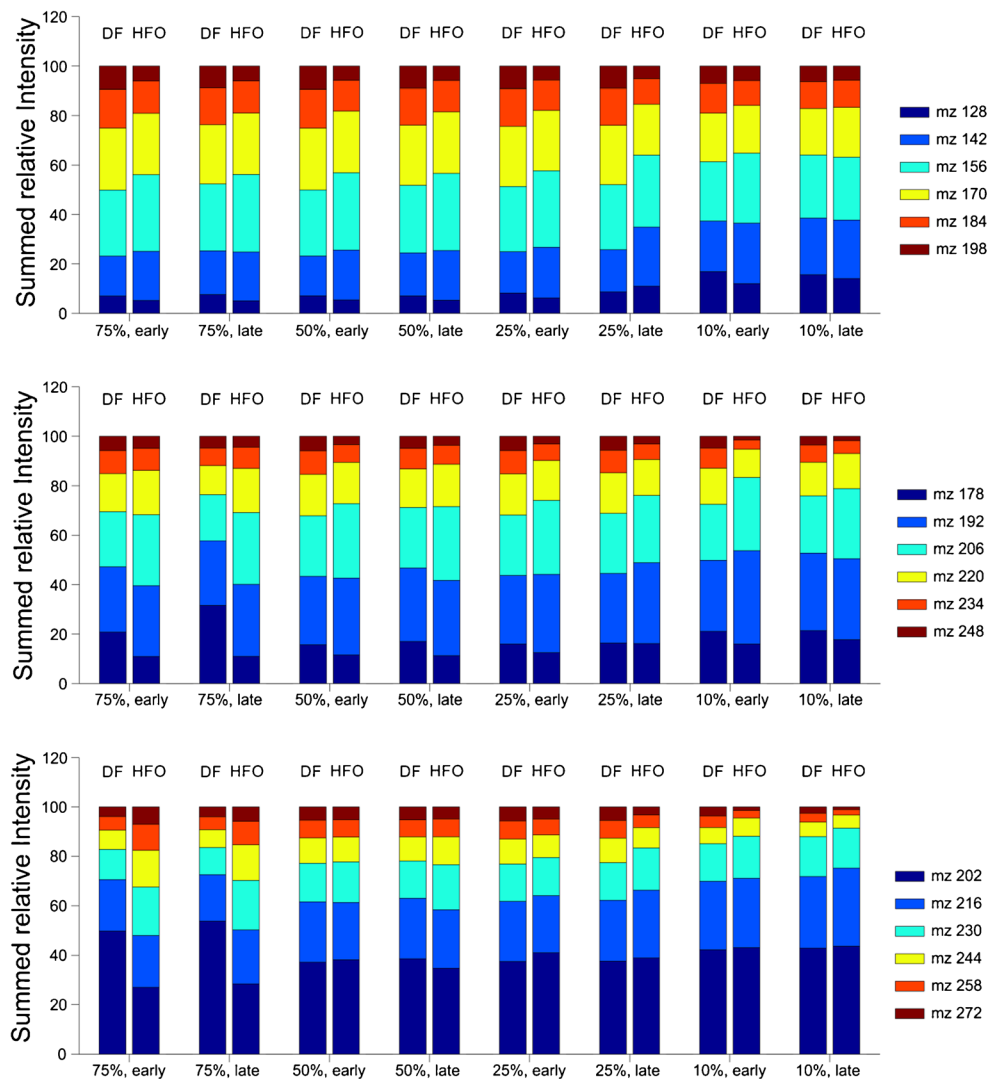


Table 3 Emission factors during the engine cold start with diesel fuel for selected aromatic compounds. The values are averages of three engine start experiments

Toluene [mg/kWh]	Phenol [mg/kWh]	Naphthalene [mg/kWh]	Me-naphthalene [mg/kWh]	Phenanthrene [μ g/kWh]	Pyrene [μ g/kWh]
13.3 \pm 2.2	16.1 \pm 0.2	4.5 \pm 1.7	6.1 \pm 2.7	43 \pm 38	144 \pm 95

naphthalene, methyl naphthalene and their higher alkylated derivatives [17] which can lead to increasing values at poorer combustion conditions.

The comparison of the normalised phenanthrene data displays some differences between DF and HFO exhaust. While at high (75 %) and medium (50 %) power of the engine the signal intensities are almost similar in HFO exhaust, there are larger variations in DF exhaust (see Fig. 4). There are also larger differences between pyrene data of the diesel and heavy fuel exhaust for high power engine conditions (75 %), but the differences for lower engine loads are not significant for both fuels.

With the aid of the already mentioned ionisation cross sections of toluene, phenol, naphthalene, methyl naphthalene, phenanthrene and pyrene, semi-quantification was performed for the engine start phase (averaged over 100 s after start of the engine) and various loads at DF and HFO operation. The six compounds were selected for the quantification because they

represent some typical combustion products and show high signal intensities for almost all performed measurements, and the assignment is unambiguous (the ionisation cross section of the two methyl naphthalene isomers should not differ significantly).

Since the engine start is a very transient process, the initial conditions (e.g. temperature of lubricating oil and introduced fuel) must be kept constant to reach reproducible measurements. On the test bench, all conditions were manually adjusted, which can lead to a certain variability of the emitted amounts of the exhaust gas. The starting phase of the engine has been defined as the first 100 s after engine start and the shown emission rates are averaged over that period. In Table 3, the averaged concentrations per engine energy output of some typical combustion products for engine cold start with diesel fuel are given. Especially the mono-aromatic and volatile compounds toluene and phenol show relatively high concentration values with 13.2 and 16.4 mg/kWh,

Table 4 Emission factors for selected aromatic compounds and the sum parameter THC during engine operation with diesel fuel (DF) and heavy fuel oil (HFO) given in milligrammes per kilowatt-hour and filter smoke number (FSN) without unit

Fuel	Engine power	SOI [$^{\circ}$ CA]	Tol	Phe	Naphth	Me-naphth	Phen	Py	THC	FSN
DF	100 % (80 kW)	EI	3.8	2.5	0.6	1.7	0.2	0.2	–	0.36
DF	100 % (80 kW)	LI	3.5	2.5	0.7	1.8	0.1	0.1	910	0.35
DF	75 % (60 kW)	EI	3.4	2.1	0.6	1.6	0.1	0.1	1230	0.49
DF	75 % (60 kW)	LI	4.2	2.5	0.7	1.8	0.2	0.2	1240	0.78
DF	50 % (40 kW)	EI	3.8	2.2	0.7	2.0	0.1	0.1	1270	0.37
DF	50 % (40 kW)	LI	3.3	1.8	0.6	1.9	0.1	0.1	1110	1.35
DF	25 % (20 kW)	EI	3.0	2.2	0.7	1.7	0.1	0.1	900	0.08
DF	25 % (20 kW)	LI	3.2	2.7	0.8	1.8	0.1	0.1	910	0.12
DF	10 % (8 kW)	EI	15.4	25.5	5.3	7.5	0.5	0.5	3510	0.02
DF	10 % (8 kW)	LI	36.9	59.4	11.8	20.4	1.2	1.3	8360	0.02
DF	2.5 % (2 kW)	EI	183.5	247.3	56.7	111.6	6.1	6.3	45,620	0.03
DF	2.5 % (2 kW)	LI	322.1	405.3	100.3	195.7	10.5	10.9	–	0.01
HFO	75 % (60 kW)	EI	5.6	2.8	3.1	14.0	0.8	0.7	–	0.28
HFO	75 % (60 kW)	LI	5.9	3.0	3.3	15.1	0.9	0.7	–	0.57
HFO	50 % (40 kW)	EI	4.1	2.1	2.2	9.7	0.6	0.3	740	0.21
HFO	50 % (40 kW)	LI	4.3	2.3	2.5	11.0	0.6	0.4	790	0.37
HFO	25 % (20 kW)	EI	5.5	4.4	3.3	12.8	0.8	0.4	1320	0.57
HFO	25 % (20 kW)	LI	13.3	17.4	9.3	23.6	2.2	1.1	2280	1.06
HFO	10 % (8 kW)	EI	99.4	137.4	65.2	155.8	19.6	8.4	13,100	2.15
HFO	10 % (8 kW)	LI	99.4	104.6	60.5	119.5	15.6	7.4	17,990	–

SOI start of injection, EI early injection, LI late injection, Tol toluene, Phe phenol, Naphth naphthalene, Me-naphth methyl naphthalene, Phen phenanthrene, Py pyrene, THC total hydrocarbons, FSN filter smoke number

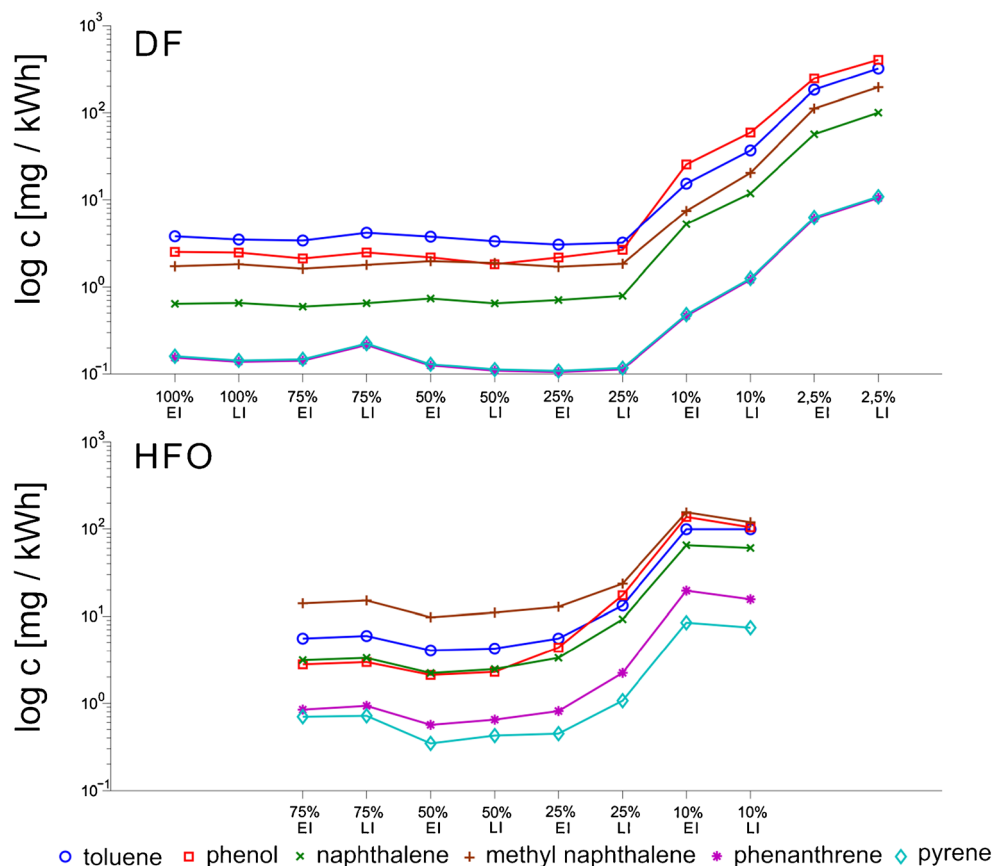
respectively, for the cold start of the engine with diesel fuel. The emission factors for the two selected bi-cyclic aromatic compounds naphthalene and methyl naphthalene were 4.5 and 6.1 mg/kWh engine energy output, respectively. Poly-aromatic compounds with three and four rings such as phenanthrene and pyrene are emitted in only small amounts in comparison to the mono-aromatic and bi-cyclic compounds. The large quantities of the mono-aromatic and bi-cyclic compounds in comparison to the PAHs with three or four rings indicate that during the initial phase of the engine operation, the proportion of unburned to thermally decomposed and partially oxidised fuel is much higher than for stable combustion conditions. Figure 2 (bottom) also illustrated a short increase of the signal intensity for toluene and naphthalene directly after starting the engine, but only a slow increase in signal intensity of phenanthrene and pyrene which indicates the pyrogenic origin of these compounds. Another reason for the only slight increase of compounds with more than two fused benzene rings are the lower vapour pressures of these compounds, which especially during engine start-up can lead to adsorption of these compounds on cold surfaces in the engine. In contrast, toluene and naphthalene originate from evaporated unburned fuel.

Table 4 illustrates the averaged concentrations of the abovementioned compounds at different engine loads and SOI. Highest emission rates of almost all organic compounds

and the sum parameter THC were measured for idling (measured only for DF operation) and low power conditions of both operation modes. Operation with diesel fuel at maximum, high and medium power shows only minor differences of the emission rates (Table 4). The same holds true for high and medium power at heavy fuel oil operation mode. At 25 % engine load for heavy fuel oil and low power (10 %) for diesel fuel, there are greater differences between early and late start of injection. It is not yet clear what the cause of that deviation is because a poorer, more unstable and more incomplete combustion condition at low loads applies to both early and late injection. Figure 5 shows once more the behaviour of increasing emission factors of both fuels with decreasing engine power and the increasing differences for early and late SOI at low power conditions. The calculated HFO emission factors of naphthalene, phenanthrene and pyrene (Table 4) are in most cases in good agreement with the measured offline data of Agrawal et al. [10].

A comparison of the emission rates of toluene for both fuels shows only minor differences for both injection times at high and medium power and for the early injection at low power conditions. Due to the more unstable combustion conditions, the differences become more significant for lower load levels (see Table 4). For the PAHs naphthalene, methyl naphthalene, phenanthrene and pyrene, the differences between HFO and DF operation emission factors are much more

Fig. 5 Logarithmic emission factors of toluene, phenol, naphthalene, methyl naphthalene, phenanthrene and pyrene for diesel fuel (*top*) and heavy fuel oil (*bottom*) operation at different engine loads and SOI



apparent, especially in the case of phenanthrene where the emission rates are larger for HFO by a factor of 4.5 (75 %, late injection) to 39 (10 %, early injection). For the formation of aromatic species during combustion, two processes play an important role: on the one hand, the direct emission of unburned fuel components [35] and, on the other hand, the pyrosynthesis (formation of aromatics by regeneration of fragmented radical species). Rhead and Hardy [36] reported that both mechanisms, the survival of the fuel components and the pyrosynthesis, play a role in PAH formation. Due to the fact of a higher exhaust temperature for the high power conditions (approximately 415 °C for DF and 400 °C for HFO) compared to low power conditions (240 °C (DF), 280 °C (HFO)), the pyrogenic pathway seemed to be the more important process at high engine loads.

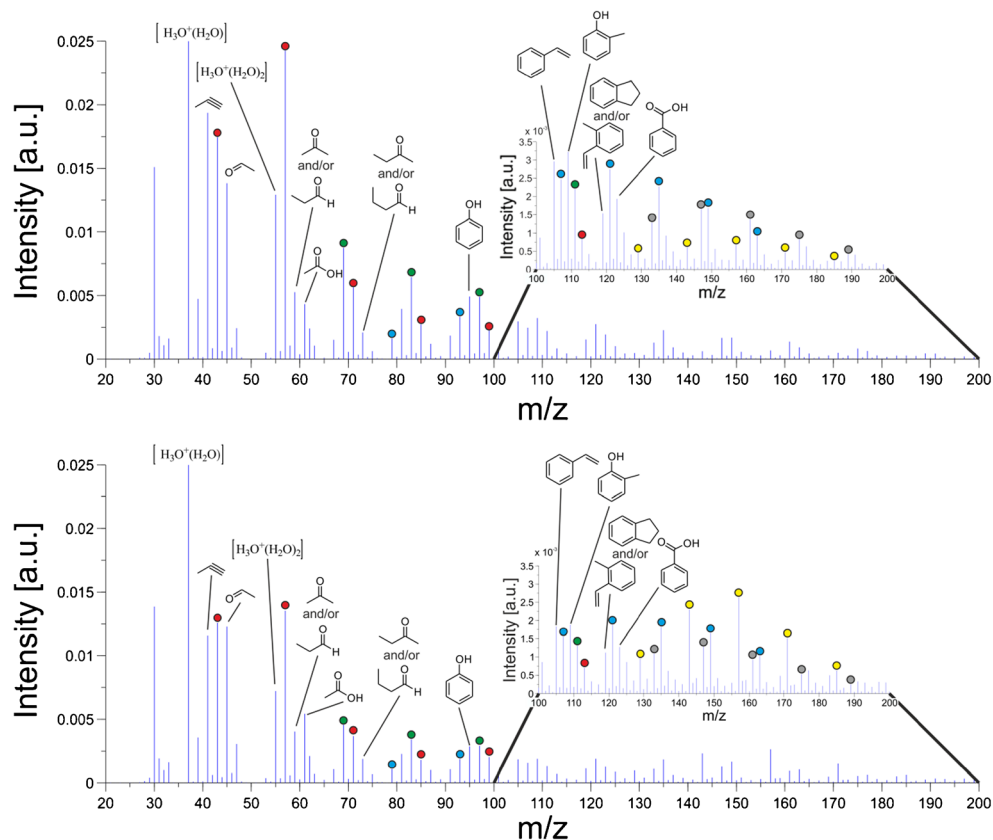
Table 4 also shows the filter smoke number (FSN) which gives information about filter paper blackening caused by a sample gas volume drawn through a filter paper. The FSN is measured by light absorption changes in reflection and the larger the number the darker the filter. There are some differences between early and late SOI for both fuels with in most cases higher values for late injection setting, which means more soot on the filter. For 75 and 50 % engine loads, the FSN for diesel fuel operation is higher than for HFO, but at lower loads, one can observe a significant decrease of the FSN for DF and a sharp increase of the smoke number for HFO.

Especially for diesel fuel, the behaviour of the FSN is in contrast with the calculated gas phase emissions, which are increasing with lower engine loads.

The PTR mass spectra depicted in Fig. 6 show signals on almost every odd mass in a range between m/z 20 and m/z 200. The odd numbered masses are due to protonation of the molecules, present in the form $[M+H]^+$. The highest intensity at m/z 37 in both spectra belongs to the water cluster $[H_3O^+(H_2O)]$, and the mass to charge ratio 55 is represented by $[H_3O^+(H_2O)_2]$. Due to this, it is not possible to make any statements about the occurrence of the toxic and carcinogenic compound 1,3-butadiene, which is known to be present in the exhaust of diesel fuel [17, 37, 38]. All other compounds which are visible in the mass spectra are derived mainly from oxygenated species (alcohols, acids, aldehydes and ketones), alkenes and aromatic hydrocarbons.

Dominant signals appear for various engine loads and operation modes at m/z 30, 41, 43, 45 and 57, respectively. Due to high NO concentrations in the exhaust gas, it is assumed that the signal at m/z 30 belongs to a single positive-charged nitric oxide as a constant interference signal and probably formed by charge transfer with positive-charged oxygen ions (formed as an impurity of primary H_3O^+). Jobson et al. [19] reported in an earlier study about diesel exhaust measurements with PTR-MS that the masses at m/z 43, 57, 71, 85 and 99 are fragments, which are derived from long-chained

Fig. 6 PTR mass spectra of DF exhaust (top) and HFO exhaust (bottom) at 40 kW (50 %) engine power over 20 full scan mass spectra. Red circles—alkenes and/or alkane fragments, green circles—alkynes and/or n-aldehyde fragments, blue circles—homologous series of benzene, yellow circles—homologous series of naphthalene, grey circles—homologous series of styrene (from m/z 105) and benzofuran (from m/z 119)



(C₁₀ to C₂₀) alkanes and iso-alkanes. Signals at m/z 69, 73, 83, 97 and 111 mainly belong to fragments of C₅ to C₉ n-aldehydes [19]. Nonetheless, smaller compounds such as alkenes are present as molecular protonated ions with the same m/z ratio and, thus, also are a part of the respective signals. However, the relation between fragment and molecular ions is unknown. Peak assignment was done with the aid of already published literature [16–18] and knowledge about proton affinities [39, 40], because in that case, ionisation is only possible for compounds with higher proton affinities than water. Due to the assumed fragmentation, no quantitative statements on the emission rates of the above stated masses can be given. Nevertheless, the masses at m/z 41, 43, 45 and 57 can be assigned to propyne, propene, acetaldehyde and butene and/or acrolein, respectively [16–18, 39, 40]. Especially short-chained alkenes up to C₉ are typical intermediates of the combustion of aliphatic hydrocarbons and, due to that, very prominent in the obtained mass spectra.

For compounds with the same nominal mass, e.g. acetone and propionaldehyde (m/z 59), quantitative conclusions are also difficult, although it is known that acetone is formed in higher amounts during diesel operation than propionaldehyde [10, 16, 17]. Agrawal et al. [10] have also reported about higher emission rates of acetone in comparison to propionaldehyde in HFO exhaust for low and medium power, but they have measured larger amounts of propionaldehyde for high power engine conditions.

The signal for acetaldehyde at m/z 45 is free from isobaric compounds; therefore, a calculation of emission rates was done in the same way as the already mentioned method for semi-quantification of the REMPI technique. For the sum of acetone and propionaldehyde, the emission rates were also calculated. In earlier studies, high emissions of the carbonyl compounds formaldehyde, acetaldehyde, propionaldehyde and acetone were reported [16, 17, 19, 41]. Especially formaldehyde and acetaldehyde are classified as air toxics with high reactivity, and it is supposed that they play an important role in the formation of secondary organic aerosols (SOA). Detection of formaldehyde is difficult with the used setup because of the very similar proton affinities of water and formaldehyde. On the other hand, acetaldehyde is very prominent at all different load levels. High emission rates were found for the starting phase of the engine with an averaged emission of 469 mg/kWh (averaged over ten full scale mass scans). With 193 mg/kWh, the sum of acetone and propionaldehyde also shows relatively high emission rates shortly after starting the engine. The more volatile compounds show the same trend as the mono-aromatic and poly-aromatic compounds with increasing signal intensities in accordance with decreasing engine loads (see Table 5). At low power and idling conditions, acetaldehyde also has higher emission rates with a late SOI (e.g. 76.02 and 769.72 mg/kWh for early and late injection at 10 % engine load) as the aromatic compounds

Table 5 Averaged emission factors of acetaldehyde and the sum of acetone and propionaldehyde in milligrammes per kilowatt-hour for different loads at DF and HFO operation

Fuel	Engine power [kW]	SOI [°CA]	Acetaldehyde	Σ Acetone + propionaldehyde
DF	25 % (20 kW)	EI	20.40	26.14
DF	25 % (20 kW)	LI	23.63	10.83
DF	10 % (8 kW)	EI	76.02	32.44
DF	10 % (8 kW)	LI	769.72	414.10
DF	2.5 % (2 kW)	EI	4598.76	3115.62
DF	2.5 % (2 kW)	LI	9862.49	7614.65
HFO	75 % (60 kW)	EI	6.60	4.38
HFO	75 % (60 kW)	LI	6.14	4.07
HFO	50 % (40 kW)	EI	11.14	7.17
HFO	50 % (40 kW)	LI	5.99	3.79
HFO	25 % (20 kW)	EI	12.65	8.17
HFO	25 % (20 kW)	LI	–	–
HFO	10 % (8 kW)	EI	–	–
HFO	10 % (8 kW)	LI	478.84	310.54

SOI start of injection, EI early injection, LI late injection

listed in Table 4. The high concentration of acetaldehyde at low power engine conditions is due to the strong temperature dependency of aldehyde formation. Wagner and Wyszynski reported that aldehyde formation in general takes place preferably at low temperatures [42] as it is the case at engine start and low power service.

Conclusion

The two used measurement instrumentations, REMPI and PTR mass spectrometry, have shown that they are particularly suitable methods for online monitoring of organic combustion compounds which are produced during operation of a combustion source such as a medium-speed ship diesel engine. With the two systems, we are capable to detect on the one hand (poly) aromatic compounds with high selectivity (REMPI TOF MS) and on the other hand a wide range of more volatile aliphatic and carbonylic organic compounds (PTR-QMS). The time resolution of 1 Hz (one mass spectrum per second) of the multiphoton ionisation mass spectrometer enables observing rapid changes of the combustion conditions in the engine, e.g. the engine start or the switchover of different load levels. During start-up of the engine, the appearing compounds are mainly derived from the unburned fuel. In general, low volatile organic compounds appear slightly earlier than larger species such as three- and four-ring PAH. Those compounds are formed during combustion and appear slightly delayed after engine start-up with a steady increase in the signal intensity up to a certain boundary value.

The PTR mass spectrometer used in scan mode provides a good overview of almost all organic compounds with proton affinities larger than water. Especially in the lower mass range up to m/z 100, many small combustion-derived products can be observed, e.g. acetaldehyde or the homologous series of the alkenes from C_3 up to C_7 . In general, there is a higher signal intensity of almost all low volatile organic compounds in the diesel exhaust compared to HFO exhaust. That is due to a higher proportion of aliphatic and more volatile compounds in diesel fuel. The relatively high signal intensities for the naphthalene derivatives are due to the higher aromatic content of the HFO. For almost all PAHs, the highest signal intensities were found for the alkylated ones, e.g. the C_3 -alkylated naphthalene derivatives in both fuels. The different behaviour of pyrene exhibiting the highest intensities within its homologous series at all different load levels is due to the combustion temperature and the resulting displacement of the gas phase/particle phase equilibrium, and with increasing masses, there is also an increase of the compounds in the particulate phase. A wide range of knowledge about the gaseous organic combustion products is necessary because many substances are suspected to exhibit health-relevant effects and to cause cancer.

The presented results showed in general increasing signal intensities for lower engine loads and, in almost all cases, higher emissions for HFO compared to DF. Low engine load conditions describe typical harbour manoeuvring of ships, and therefore, it is necessary to strengthen measures to reduce emissions especially at low engine loads in order to better protect coastal areas and the vicinity of ports. The results have shown that the implementation of SECAs will not only lead to reduced SO_x emissions after switchover from HFO to DF operation, but in most cases also to decreased organic exhaust emissions, in particular for (poly-cyclic) aromatic compounds such as naphthalene, phenanthrene and pyrene.

Acknowledgments Funding by the Helmholtz Foundation for the HICE Virtual Institute (www.hice-vi.eu) is gratefully acknowledged.

References

- Corbett JJ, Koehler HW (2003) *J Geophys Res D Atmos* 108:ACH 9-1-ACH 9-15
- Corbett JJ, Winebrake JJ, Green EH, Kasibhatla P, Eyring V, Lauer A (2007) *Environ Sci Technol* 41:8512-8518
- Eyring V, Isaksen ISA, Bernsten T, Collins WJ, Corbett JJ, Endresen O, Grainger RG, Moldanova J, Schlager H, Stevenson DS (2010) *Atmos Environ* 44:4735-4771
- Endresen O, Sørsgård E, Sundet JK, Dalsøren SB, Isaksen ISA, Berglen TF, Gråvir G (2003) *J Geophys Res D Atmos* 108:ACH 14-1-ACH 14-22
- Saxe H, Larsen T (2004) *Atmos Environ* 38:4057-4067
- Eyring V, Köhler HW, Van Aardenne J, Lauer A (2005) *J Geophys Res D Atmos* 110:171-182
- Smith TWP, Jalkanen JP, Anderson BA, Corbett JJ, Faber J, Hanayama S, O'Keeffe E, Parker S, Johansson L, Aldous L, Raucchi C, Traut M, Ettinger S, Nelissen D, Lee DS, Ng S, Agrawal A, Winebrake JJ, Hoen M, Chesworth S, Pandey A (2014) Third IMO GHG study 2014. International Maritime Organization (IMO), London
- Sinha P, Hobbs PV, Yokelson RJ, Christian TJ, Kirchstetter TW, Bruintjes R (2003) *Atmos Environ* 37:2139-2148
- Capaldo K, Corbett JJ, Kasibhatla P, Fischbeck P, Pandis SN (1999) *Nature* 400:743-746
- Agrawal H, Welch WA, Miller JW, Cocker DR (2008) *Environ Sci Technol* 42:7098-7103
- Sippula O, Stengel B, Sklorz M, Streibel T, Rabe R, Orasche J, Lintelmann J, Michalke B, Abbaszade G, Radischat C, Gröger T, Schnelle-Kreis J, Harndorf H, Zimmermann R (2014) *Environ Sci Technol* 48:11721-11729
- Cooper DA (2003) *Atmos Environ* 37:3817-3830
- Fridell E, Steen E, Peterson K (2008) *Atmos Environ* 42:1160-1168
- Fu M, Ding Y, Ge Y, Yu L, Yin H, Ye W, Liang B (2013) *Atmos Environ* 81:222-229
- Kasper A, Aufdenblatten S, Forss A, Mohr M, Burtscher H (2007) *Aerosol Sci Technol* 41:24-32
- Siegl WO, Hammerle RH, Herrmann HM, Wenclawiak BW, Luers-Jongen B (1999) *Atmos Environ* 33:797-805
- Schauer JJ, Kleeman MJ, Cass GR, Simoneit BRT (1999) *Environ Sci Technol* 33:1578-1587
- Cooper DA, Peterson K, Simpson D (1996) *Atmos Environ* 30:2463-2473
- Jobson BT, Alexander ML, Maupin GD, Muntean GG (2005) *Int J Mass Spectrom* 245:78-89
- Adam TW, Chirico R, Clairotte M, Elsasser M, Manfredi U, Martini G, Sklorz M, Streibel T, Heringa MF, Decarlo PF, Baltensperger U, De Santis G, Krasenbrink A, Zimmermann R, Prevot ASH, Astorga C (2011) *Anal Chem* 83:67-76
- Adam TW, Clairotte M, Streibel T, Elsasser M, Pommeres A, Manfredi U, Carriero M, Martini G, Sklorz M, Krasenbrink A, Astorga C, Zimmermann R (2012) *Anal Bioanal Chem* 404:273-276
- Butcher DJ, Goeringer DE, Hurst GB (1999) *Anal Chem* 71:489-496
- Sarvi A, Fogelholm CJ, Zevenhoven R (2008) *Fuel Process Technol* 89:510-519
- Sarvi A, Fogelholm CJ, Zevenhoven R (2008) *Fuel Process Technol* 89:520-527
- Boesl U, Zimmermann R, Weickhardt C, Lenoir D, Schramm KW, Kettrup A, Schlag EW (1994) *Chemosphere* 29:1429-1440
- Heger HJ (1999) *Anal Chem* 71:46-57
- Boesl U, Neusser HJ, Schlag EW (1981) *Chem Phys* 55:193-204
- Schwoebel H, Schubert R, Sklorz M, Kischkel S, Zimmermann R, Schubert JK, Miekisch W (2011) *Anal Bioanal Chem* 401:2079-2091
- De Gouw J, Warneke C, Karl T, Eerdekens G, Van der Veen C, Fall R (2003) *Int J Mass Spectrom* 223-224:365-382
- De Gouw J, Warneke C (2007) *Mass Spectrom Rev* 26:223-257
- Hansel A, Jordan A, Holzinger R, Prazeller P, Vogel W, Lindinger W (1995) *Int J Mass Spectrom Ion Processes* 149-150:609-619
- Zielinska B, Sagebiel JC, Harshfield G, Gertler AW, Pierson WR (1996) *Atmos Environ* 30:2269-2286
- Khalilil NR, Scheff PA, Holsen TM (1995) *Atmos Environ* 29:533-542
- Cooper DA (2001) *Atmos Environ* 35:4189-4200
- Williams PT, Abbass MK, Andrews GE, Bartle KD (1989) *Combust Flame* 75:1-24
- Rhead MM, Hardy SA (2003) *Fuel* 82:385-393
- Schmitz T, Hassel D, Weber FJ (2000) *Atmos Environ* 34:4639-4647
- Ogawa H, Li T (2011) *Int J Engine Res* 12:30-40
- Lias SG, Liebman JF, Levin RD (1984) *J Phys Chem Ref Data* 13:695-808

40. Hunter EPL, Lias SG (1998) *J Phys Chem Ref Data* 27:413–656
41. Reda AA, Schnelle-Kreis J, Orasche J, Abbaszade G, Lintelmann J, Arteaga-Salas JM, Stengel B, Rabe R, Harndorf H, Sippula O, Streibel T, Zimmermann R (2014) *Atmos Environ* 94:467–478
42. Wagner T (1996) *P I Mech Eng D J Aut* 210:109–122